

3-Dimensional Neutral Particle Transport Analysis in Heliotron J

S. Kobayashi¹, S. Nakazawa², H. Kawazome², H. Arimoto², T. Mizuuchi¹, H. Yamazaki²,
 K. Takahashi², Y. Suzuki², Y. Nakashima³, Y. Nakamura², K. Nagasaki¹, H. Okada¹,
 S. Yamamoto¹, K. Kondo² and F. Sano¹

1. Institute of Advanced Energy, Kyoto University, Uji, Kyoto 611-0011, Japan
2. Graduate School of Energy Science, Kyoto University, Uji, Kyoto 611-0011, Japan
3. Plasma Research Center, University of Tsukuba, Tsukuba, Ibaraki 305-8577, Japan

1. Introduction

In magnetized plasmas, particle balance including wall recycling is important subject for the control of plasma density and quantitative estimation of pumping capacity.[1-4] The particle balance is usually examined by means of additional gas fueling experiment or neutral particle transport analysis. In non-symmetrical systems, such as stellarator or helical devices, it is difficult to evaluate the neutral particle transport because the analysis with the assumption of toroidal symmetry cannot explain the actual experimental condition. Recently, in some non-symmetrical devices, three dimensional neutral particle transport has been carried out [2,3] using Monte-Carlo simulation code [4,5]. To understand the edge plasma physics including atomic and molecular physics, analysis on the neutral particle transport is also important issue [6-8].

In this study, we report the analysis of the neutral particle transport in Heliotron J[9]. The Heliotron J plasma has three dimensionally structure of magnetic surface and vacuum vessel. Therefore, the neutral hydrogen density using the three dimensional plasma mesh model is calculated by comparing the H α emission measurement with the simulation. The particle balance in ECH plasmas in Heliotron J is discussed from the estimation of the wall-recycling rate.

2. Experimental apparatus and neutral particle transport simulation

Heliotron J is the helical-axis heliotron device with L/M = 1/4 helical winding coil, where L and M are the pole number of the helical coil and pitch number of the field along the toroidal direction, respectively. The major and minor radius are 1.2 and 0.2 m and

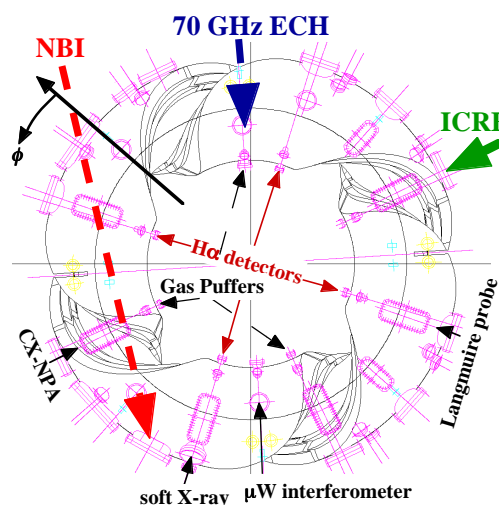


Fig.1 Top view of the Heliotron J device, heating systems and diagnostics.

the edge iota is 0.56 in the standard configuration. Figure 1 shows the top view of the Heliotron J device including heating systems and diagnostics. The plasma is produced and heated by the 70 GHz 2nd harmonic electron cyclotron resonance heating (ECH) system with maximum power of 0.4 MW. The additional heating is available with NBI (0.7 MW) or ICRF (0.4 MW).

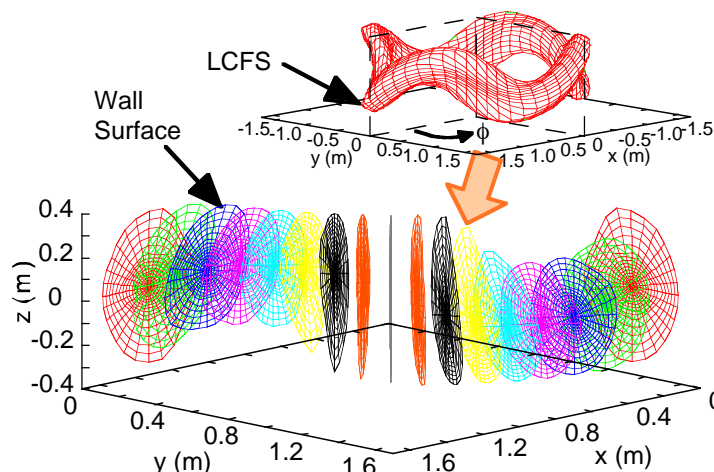


Fig. 2 Bir's-eye view of the plasma mesh model used in the DEGAS simulation. This model has 64 and 28 zones in toroidal and poloidal direction, respectively.

In order to simulate the neutral transport in the Heliotron J plasma, the DEGAS code is employed[4,5]. The plasma mesh model is constructed using the puncture plots of the magnetic field line calculated by the KMAG code.[10] Figure 2 shows the schematic view of the plasma mesh model used in the simulation, where the upper figure illustrates the last closed flux surface (LCFS) and the bottom is poloidal cross section at each toroidal angle ($0^\circ < \phi < 90^\circ$). This mesh model has 64 and 28 zones in toroidal and poloidal directions, respectively. The plasma parameters are given using the experimental results. i.e. the microwave interferometer and Langmuire probe is used to determine the density, soft X-ray detector with absorption method is for the electron temperature and the charge-exchange neutral particle analyser for the ion temperature.

3. Calculation results

The neutral particle simulation in the 70 GHz ECH plasma is performed using two particle sources. One is gas puffing from the gas injectors and the other is hydrogen recycling from the wall surface. In this calculation, the particle source distribution of the hydrogen recycling (H_2) from the wall surface is assumed to be uniform having the initial velocity at the wall temperature. In the standard configuration of Heliotron J, the structure of edge magnetic field is complicated since it is strongly affected by "natural-islands" near the outermost magnetic surface having $m/n = 7/4$ structure (cf. edge iota ~ 0.56). Then it is difficult to model a plasma mesh for the neutral transport simulation in the region outside the LCFS of Heliotron J. In this study, we used a simplified mesh model for the outside LCFS.

Figure 3 shows the contour plots of the atomic hydrogen density deduced from the simulation at the toroidal angle $\phi = 33.75$ deg. and 78.85 deg., respectively. The fueling rate from the wall recycling is determined so as to reproduce the toroidal

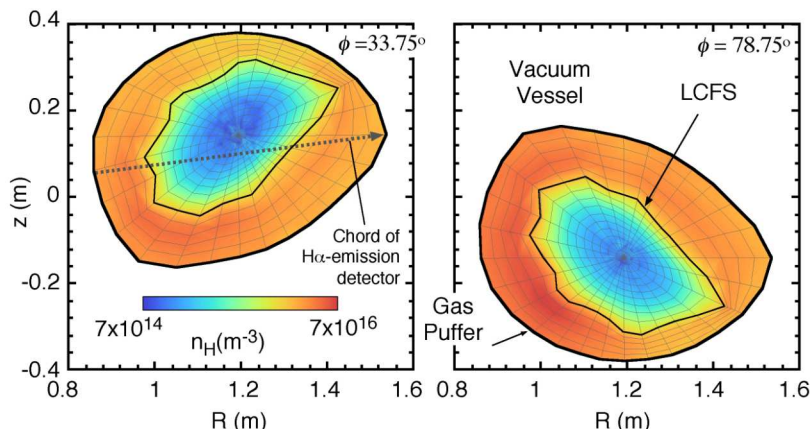


Fig. 3 Contour plot of the atomic hydrogen density deduced from the DEGAS simulation in the Heliotron J ECH plasma in the case of the line-averaged electron density of $0.9 \times 10^{19} \text{ m}^{-3}$.

profile of the measured $\text{H}\alpha$ -emission intensity. In this calculation, the recycling rate, Q_{WR} , was assumed to be $8.7 \text{ Pa m}^3/\text{s}$, while the gas puffing rate, Q_{GP} , was set to be $0.5 \text{ Pa m}^3/\text{s}$. From the simulation the neutral hydrogen density around the gas puffer is relatively higher than the other region by a factor of two.

The toroidal profile of the atomic hydrogen density averaged inside LCFS deduced from the simulation is compared with that estimated from the $\text{H}\alpha$ -emission measurement, which is shown in Fig. 4. The simulation results in the cases of only gas puffing or wall recycling are also shown in the figure. The profile from the measurement can almost be explained by the simulation using the two sources. The difference in both densities at $\phi = 220^\circ$ may be ascribed to the ambiguity of the measurement or uncertainty in the input parameters for the simulation. Although the further development is needed to model more precise edge magnetic structure and to measure a detailed poloidal profile of the $\text{H}\alpha$ -emission intensity, this method enables us to estimate the fueling rate from wall recycling.

4. Discussion

Using the above method, we estimate the particle balance in various density cases in ECH plasmas of Heliotron J. Figure 5 shows the dependence of the fueling balance on the line-averaged electron

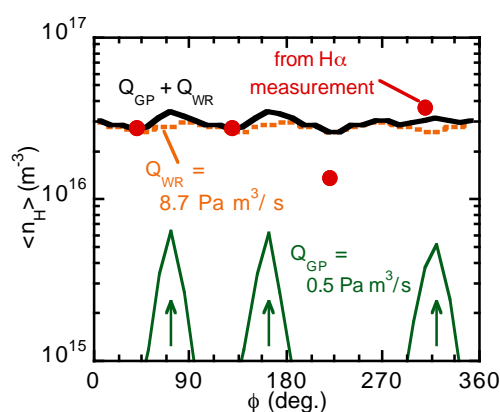


Fig. 4 Toroidal profile of the neutral hydrogen density deduced from the simulation and $\text{H}\alpha$ -emission measurement. The narrow-solid, dashed and bold-solid lines show the calculation results using the gas puffing, wall recycling and both sources, respectively. The location of each gas injector is shown by the arrow.

density calculated by the simulation. As shown in the figure, the fueling ratio of the wall recycling to the gas puffing increases with the density in the density range up to $1 \times 10^{19} \text{ m}^{-3}$. When the density is more than $1 \times 10^{19} \text{ m}^{-3}$, on the other hand, the ratio is almost unchanged with the density. In this density range, it is found that the global particle confinement time, defined by N/S , where N and S are the total electron number and particle source integrated within LCFS, respectively, increases with the density.

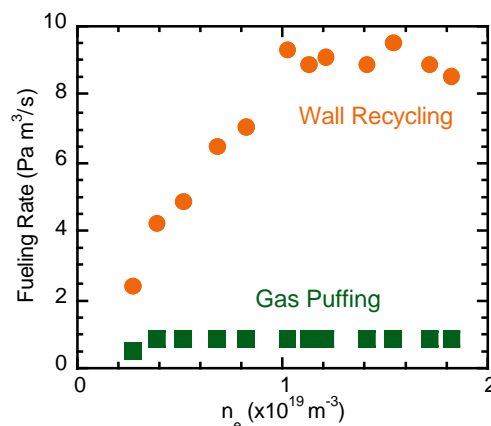


Fig.5 Dependence of the particle balance on the line-averaged electron density in 70 GHz ECH plasmas.

5. Summary

We analyzed the neutral particle transport in the Heliotron J plasmas by means of the combination of the $\text{H}\alpha$ emission measurement and Monte-Carlo simulation taking into account of the three dimensional shape of the magnetic surface and vacuum vessel. From the neutral particle transport analysis, we could evaluate the fueling rate from the wall recycling. In the 70 GHz ECH plasmas in Heliotron J, it was found that the wall recycling increased with the line-averaged density in the density range up to $1 \times 10^{19} \text{ m}^{-3}$, while the wall recycling is almost unchanged in the case of $1 \times 10^{19} \text{ m}^{-3} < n_e < 2 \times 10^{19} \text{ m}^{-3}$. The increase in the global particle confinement time with the density was observed in the density range.

References

- [1] H. Takenaga *et al.*, *Nucl. Fusion* **39**, (1999) p1917.
- [2] Y. Nakashima, *J. Nuclear Materials* **313-316**, (2003) p553.
- [3] M. Shoji, *et al.*, *J. Nuclear Materials* **313-316**, (2003) p614.
- [4] D. P. Stotler, *et al.*, *Phys. Plasmas* **3**, (1996) p4084.
- [5] D. Heifetz, D. Post, *et al.*, *J. Comp. Phys.* **46** (1982) p309.
- [6] U. Fantz, *et al.*, *J. Nucl. Mater.* **313-316**, (2003) p743.
- [7] H. Kubo, in "ATOMIC AND MOLECULAR DATA AND THEIR APPLICATIONS", edited by D. R. Schultz, *et al.*, American Institute of Physics, New York, (2002) 161.
- [8] K. Sawada, *et al.*, *J. Appl. Phys.* **78** (1995) p2913.
- [9] T. Obiki *et al.*, *Nucl. Fusion* **44** (2004) p47.
- [10] Y. Nakamura, *et al.*, *J Plasma Fusion Res.* **69** (1993) p41.